

Pore Pressure Prediction: Implications for Overpressure and Mud Preparation in the Coastal Swamp Depobelt, Niger Delta, Nigeria

O. A. Anyiam, K. C. Offiaukwu, O. C. Ekwenye

Department of Geology, University of Nigeria, Nsukka, Nigeria

Received August 23, 2024; Accepted November 27, 2024

Abstract

Abnormal pore pressures also called overpressure is prevalent in the Cenozoic Niger Delta Basin. The Eocene to Recent sedimentary succession in the wells drilled in the area comprises sandstones of the Benin Formation overlying interbedded sands and shales of the Agbada Formation. In order to precisely predict pore pressure, this study used wireline logs from five wells located in the "ECLIPSE" field of the Coastal Swamp Depobelt. The objectives were to identify the onset of overpressures, carry out a 1D pore pressure prediction and well calibration model using wireline well logs, convert pressures to equivalent mud weight (EMW) in parts per gallon (ppg), which will be used to prepare the drilling mud program and well architecture, and to ascertain the causal mechanism of the over pressured zones in the offset wells. Based on departures from expected compaction trends, intervals of overpressure were inferred from the well logs. The results of the study reveals that the average depth of overpressure occurrence in the Coastal Swamp Depobelt is 7,500 ft. Above these depths, the wells are normally pressured and can be drilled with mud weights equal to, or slightly above 8.5 ppg. The EMW plots show four levels with varying pore pressures that can be drilled with a certain mud weight where each successive level represents intervals with pore pressure greater than the former. These levels determine the casing plan as the well needs to be cased and cemented before weighting up. The results from this study establish that the drilling window available in the study area falls between 8.5 and 15.0 ppg. Based on the cross-plots of density and velocity, it was observed that velocity increases with respect to increasing density at depths between 7,000 and 12,000 ft. This suggests that the cause of the geo-pressure is disequilibrium compaction. At depths greater than 12,000 ft, disequilibrium compaction and unloading are interpreted to cause overpressure due to a decreasing velocity against constant density trend.

Keywords: *Geo-pressure; Disequilibrium compaction; Unloading; Drilling window.*

1. Introduction

One of the key inputs to successful well planning is accurate pore pressure prediction and it is more difficult in frontier basins with complex geology and where few offset wells exist beyond known depths. Over time, overpressure in sediments has been a difficult challenge to manage resulting in problematic situations such as borehole deformation from adjusted mud weight [1]. Before drilling, pore pressure prediction ensures that the appropriate mud weight for drilling is selected by weighting up or weighting down and drill casing program to be optimized thereby enabling safe and economic subsurface drilling. The Terzaghi effective stress law, which asserts that pore pressure in the formation is a function of total stress and effective stress, is the primary theory used to predict pore pressure [2]. The importance of this information has gradually been realized as some major well disasters have caused the loss of precious human life, material and adverse publicity. Drilling non-productive time, decreased drilling speed and potentially disastrous events like well blowouts, pressure kicks, and well complexities can all be caused by inaccurately predicting overpressures before drilling, unintentional fracture of the formation and ensuing mud losses are possible minor accidents [3-5]. The oil well blowout

at Aiteo's well-1 in the Santa Barbara River, Nembe, Nigeria, attracted attention as its unending spewing caused much harm and misery in the coastal communities over the weeks since it ruptured on November 1, 2021 [6]. The aim of the study was to carry out pore pressure prediction (PPP) and interpretation in order to determine and understand the distribution of over pressured Cenozoic sediments and prepare mud program and well architecture in wells within the Coastal swamp depobelt, Niger Delta Basin, Nigeria.

2. Geology of the Niger Delta

The Niger Delta Basin, situated at the apex of the Gulf of Guinea is one of the most prolific deltaic hydrocarbon provinces in the world. The study area is the "Eclipse" field in the Coastal Swamp Depobelt of the Niger Delta Basin (Figure 1). The escalator regression model of Knox *et al.* [7] describes the one-way step-wise outbuilding of the Niger Delta through geologic time. The units of these steps are the depobelts which represent successive phases of delta growth. Over the years, these series of events have occurred five to six times, defining a number of depobelts in the Niger Delta. Five depobelts; Northern Delta, Greater Ughelli, Central Swamp, Coastal Swamp, and Offshore are usually recognized. The Niger Delta's enormous syn-sedimentary growth faults, rollover anticlines and shale diapirs are its most conspicuous structural characteristics [8]. The lithostratigraphic units that make up the stratigraphic sequence of the Niger Delta Basin comprises of a basal marine over pressured and under-compacted mobile shales, clay, and silt units of the Akata Formation [9-10], paralic succession of alternating sands and shales of the Agbada Formation and alluvial or upper coastal plain (continental) sandstone successions of the Benin Formation [11] (Figure 2).

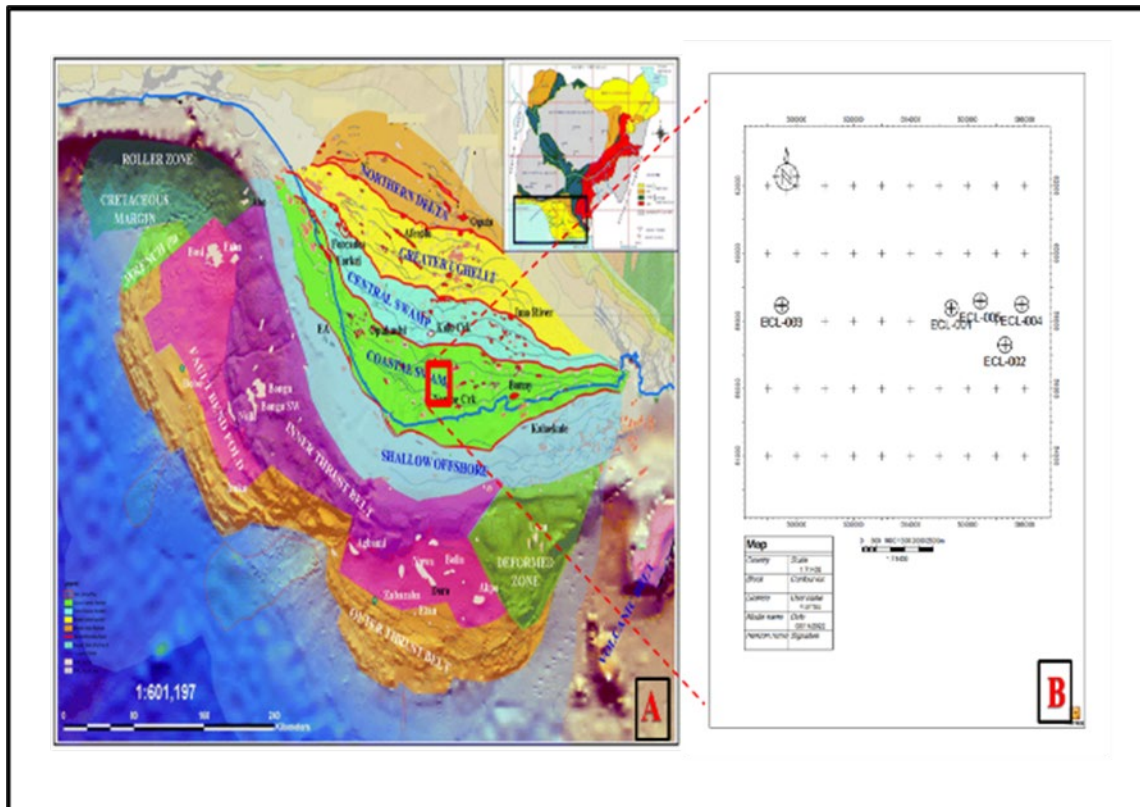


Figure 1. (A) Map of Nigeria (inset) [5], showing the location of the Niger Delta, depobelts and the study area in the Coastal Swamp Depobelt (B) Base map of the study area.

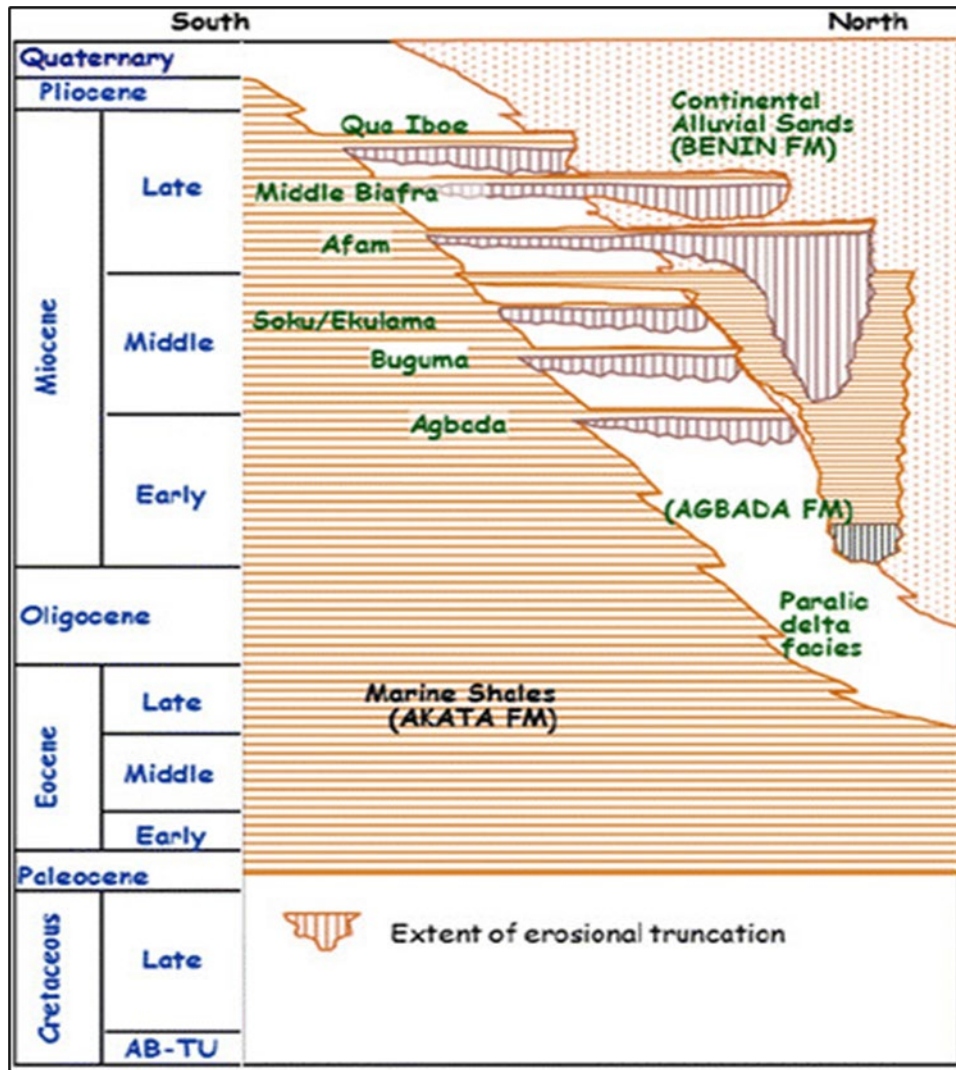


Figure 2. Regional stratigraphy of the Niger Delta Basin showing the Akata, Agbada and Benin Formations (modified [16])

3. Materials and methods

This study was carried out using data from five (5) wells in the "Eclipse" Field, Coastal swamp depobelt, Niger Delta Basin, Nigeria. The data used were well logs in American Standard Code for Information Interchange (ASCII) format. Conventional suites of well log data provided for the study are gamma ray (GR), sonic and density logs (Table 1). The study entails using wireline well logs data to produce the hydrostatic gradient, lithostatic gradient, shale normal compaction trend, fracture gradient and pore pressure prior to conversion to equivalent mud weight (EMW) in the study area.

Table 1. Wireline well log data provided for the study included gamma-ray, sonic and density logs.

WELL	GR	DEN	SONIC
ECL- 001	✓	✓	✓
ECL- 002	✓	✓	✓
ECL- 003	✓	✓	✓
ECL- 004	✓	✓	✓
ECL- 005	✓	✓	✓

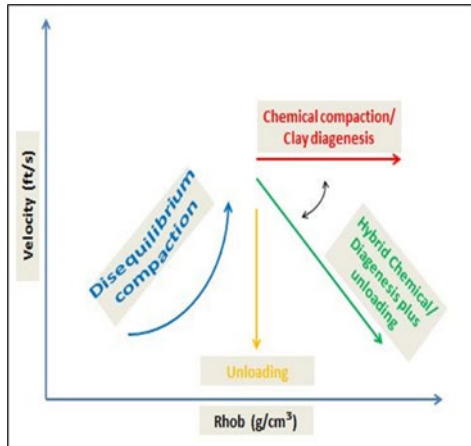


Figure 3. Schematic diagram of velocity-density cross-plot showing the possible trends for different overpressure generating mechanisms (modified after [17-18]).

$$OBG = \rho * g * ht$$

where OBG = overburden pressure, ρ = density; g = acceleration due to gravity, ht = thickness.

The pressure in the sandy reservoir is assumed to be close to the surrounding shales and pressures in shales can only be predicted but not measured [13]. The Normal Compaction Trend Line (NCTL) represents the sonic log values if the pore pressure were normal (hydrostatic). The pore pressure and fracture gradient prediction from sonic compressional transit time was derived using [14], and the empirical equation was given as (equation 3).

$$P_{shale} = OBG - \{(OBG - P_{nl}) * \left(\frac{\Delta T_n}{\Delta T_0}\right)^a\} \quad (3)$$

where P_{nl} is the P_{shale} for a hydrostatic condition; "a" which is "1.2" is a parameter calibrated within a specific basin, OBG is the lithostatic pressure, T_n is the normal transit time and T_0 is the transit time obtained from the well log. Also, Mathews and Kelly [15] established a measure of effective stress coefficient for predicting fracture gradient, which is represented by the formula (equation 4):

$$FG = K_0 (OBG - PP) + PP \quad (4)$$

where FG is the fracture gradient; PP is the pore pressure gradient; OBG is the overburden stress gradient; K_0 is the effective stress coefficient; $K_0 = \sigma_{min}' / \sigma_v'$; σ_{min}' is the minimum effective in-situ stress; σ_v' is the maximum effective in-situ stress or effective overburden stress.

The equivalent mud weight which is the overall force exerted at a true vertical depth at any given depth, represented in terms of mud density [13] was evaluated using the formula below (equation 5):

$$EMW = \frac{\rho}{g h} \quad (5)$$

Finally, the primary cause of overpressure was identified using the cross-plot of velocity vs density (Figure 4).

3. Results and discussions

3.1. Hydrostatic (normal pressure) and lithostatic pressure (overburden pressure)

In Eclipse well one (ECL-001), the water density was set at 1.03 g/cc and hydrostatic pressure ranges from 14 psi to 5,085 psi at the bottom of the well. The density curve which starts at 4,000 ft is extrapolated to the top of the well to calculate the overburden pressure with an overriding power of 12 in the shallow zones (Figure 5). Its calculated lithostatic pressure ranges from 20 psi at the surface to 10,736 psi at the bottom. Similarly, the hydrostatic

The sonic logs were de-spiked using the curve filtering process in explorationist module in order to ensure they are comprised of only proper range of values. This process uses the trimmed mean method with an appropriate operator length of 30 ft and a trim of 25%. The sonic logs were largely well smoothed (Figure 3). The hydrostatic pressure increases linearly with depth and is represented by equation 1.

$$P_w = \rho * g * h \quad (1)$$

where h , ρ and g are the height, density of fluid, and acceleration due to gravity, respectively.

Recall that at any depth, lithostatic pressure is the force created by the combined weight of the rocks and interstitial fluids [12]. It is represented by equation 2.

$$(2)$$

pressure in Eclipse well two (ECL-002) was calculated with a default water density of 1.03 g/cc and the normal pressure varies from 14 psi at the top to 6,402 psi at the base (Figure 6).

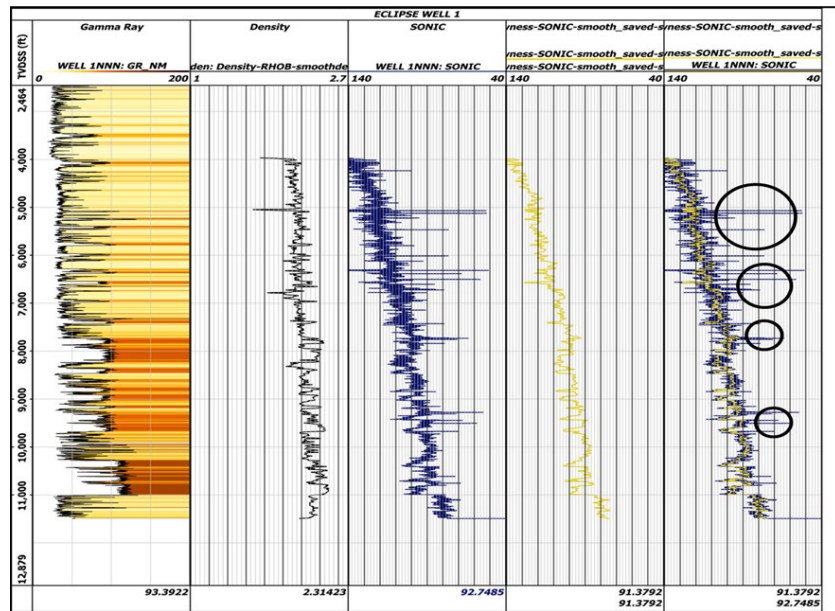


Figure 4. Track 3 indicates original sonic well curve with spikes (blue curve); Track 4 shows the de-spiked sonic well curve (yellow curve); Track 5 shows the circles representing deleted spikes in ECL - 001.

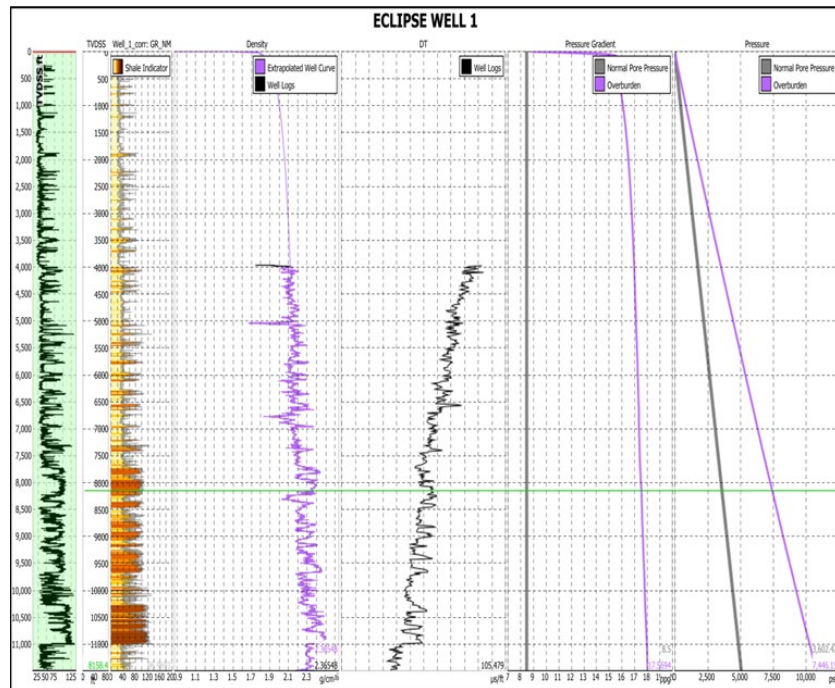


Figure 5. The normal pressure and the lithostatic pressure are shown in Track 4 and 5 in ECL - 001.

The density curve starts at a depth of 6,500 ft but the curve extrapolation to the top of the well starts at 7,000 ft due to noise. The lithostatic pressure ranges from 20 psi to 13,425 psi or 17.9 ppg at the bottom when converted to equivalent mud weight. In Eclipse well three (ECL-003), the normal pressures fall between 10 psi to 5,749 psi at the bottom of the well when sea water density of 1.03 g/cc was used. For accurate overpressure estimation, the density curve which starts at 4,000 ft is extrapolated to the top of the well with an overriding

power of 12 in the shallow zones. The overburden pressure in the well ranges from 20 psi to 12,108 psi or 18 ppg (EMW) at a depth of 13,000 ft (Figure 7). The hydrostatic pressure evaluated in Eclipse well four (ECL-004) varies from 8.8 psi to 5,545 psi at the base of the well. The density curve is extrapolated to the surface from 5,000 ft, with an overriding power of 12 and the calculated lithostatic pressure extends to 11,755 psi and 18 ppg (EMW) at the bottom of the well. More so, in Eclipse well five (ECL-005), the normal pressure varies from 6 psi to 4,360 psi at the bottom. Due to poor signal-noise ratio, between 3,000 - 3,300 ft, the density curve is extrapolated from 3,500 ft with an overriding power of 12. Lithostatic pressure ranges from 20 psi to 9,085 psi or 18 ppg (EMW) near the bottom of the well.

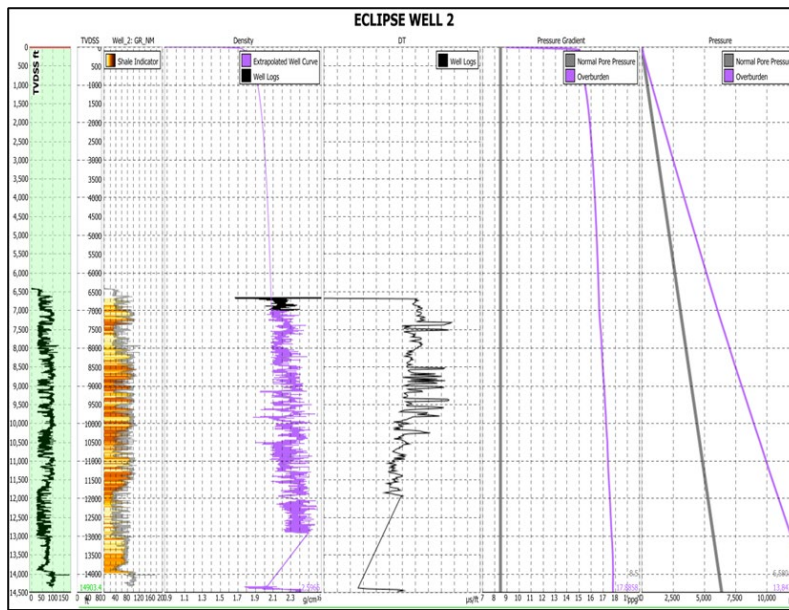


Figure 6. The normal pressure and the lithostatic pressure are shown in Track 4 and 5 in ECL – 002.

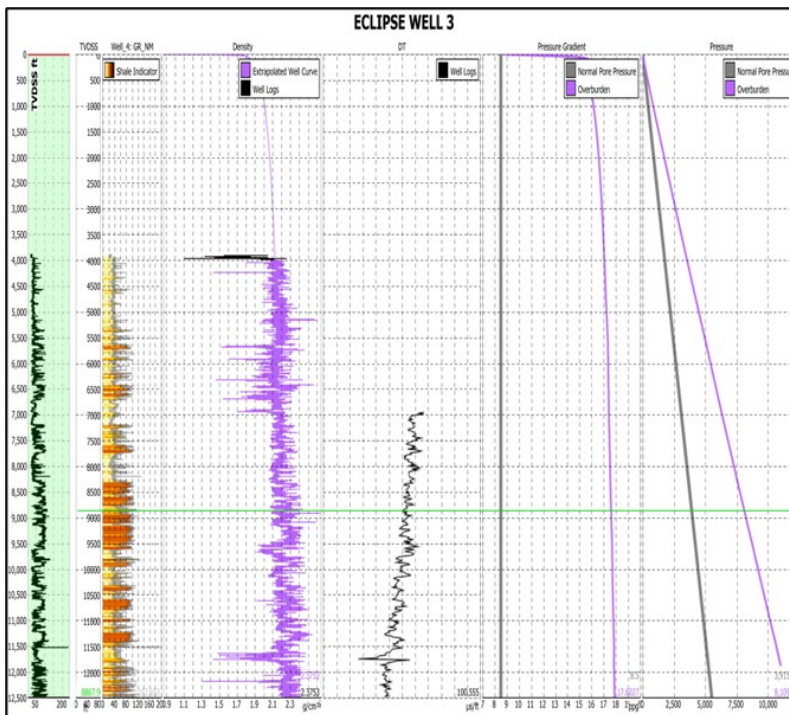


Figure 7. The normal pressure and the lithostatic pressure are shown in Track 4 and 5 in ECL – 003.

3.2. Normal compaction trend line (NCTL)

The low permeability intervals (Shales) that were isolated produced an "Observed Shale Compaction Trend" (OSCT) with a smoothing parameter of 500 ft. The normal compaction trend line plotted along this trend is referred to as the "Normal Shale Compaction Trend line" (NCTL) (Figure 8).

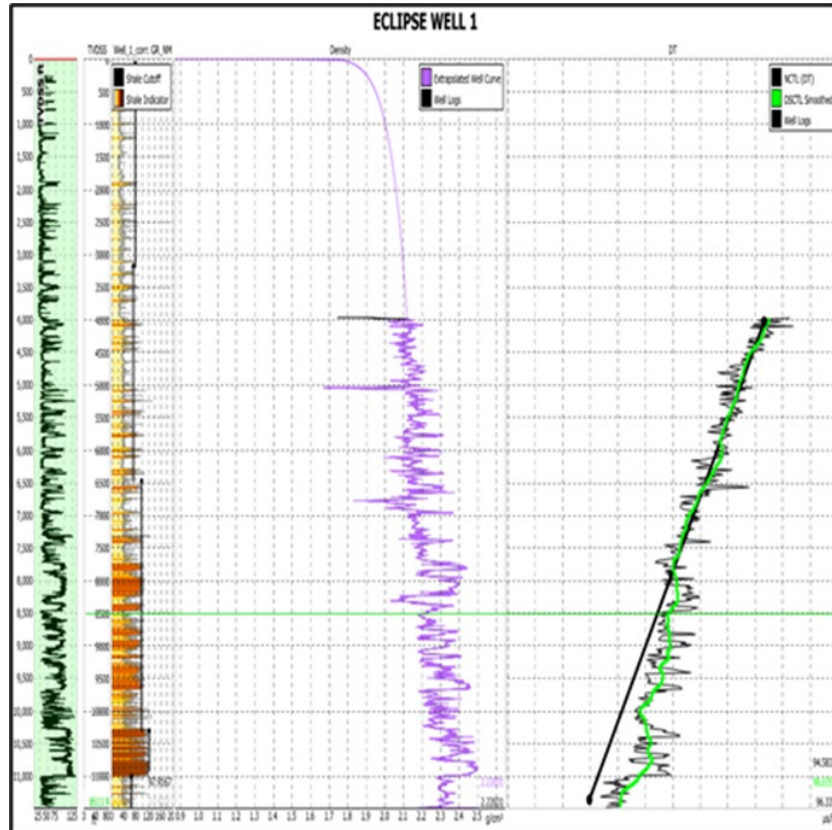


Figure 8. Track 1 shows shale cutoff zones while Track 3 shows observed shale compaction trend curve (green curve) and the black line representing the normal compaction trend line (NCTL) in ECL – 001.

3.3. Pore pressure and fracture pressure

Eclipse Well One (ECL-001): The formation pore pressure is hydrostatic (where calculated pore pressures align with the normal pressure) at a depth less than 8,000 ft which correlates with intervals where the observed shale compaction trend (OSCT) aligns with normal shale compaction trend line (NSCTL) on the sonic log. Below this depth, the formation is moderately under-compacted as indicated by the deviation of the sonic curve from the normal compaction trend, implying an increase in pore pressure (Figure 9). Between 10,000 to 11,500 ft, the observed shale compaction curve deviates further from the normal shale compaction trend line indicating elevated in-situ pore pressures due to additional under compaction. Geo-pressures observed below 8,000 ft ranges from 4,500 psi to 5,500 psi in the mildly under-compacted intervals and reach as high as 7,000 psi at the bottom of the well. The fracture pressure increases along the well paths and extends to 9,000 psi towards the bottom of the well (Figure 9).

Eclipse Well Two (ECL-002): From the observed shale compaction trend (OSCT), at shallower depths ranging from the top of the well to 8,500 ft, the pore pressure is assumed to be normal because the curve matches the normal compaction trend. Under-compacted intervals discerned by anomalies in the observed shale compaction trend (OSCT) interpreted as overpressure are observed below this depth. Below 12,000 ft, elevated pore pressure and under-compaction are observed, as the curve deviates from the normal compaction trend. Overpressure values vary from 4,000 psi to 5,500 psi and extends to about 8,000 psi at its peak

between depths of 8,500 ft and 11,000 ft. The fracture pressure which increases with depth reaches about 10,000 psi towards the bottom of the well (Figure 10).

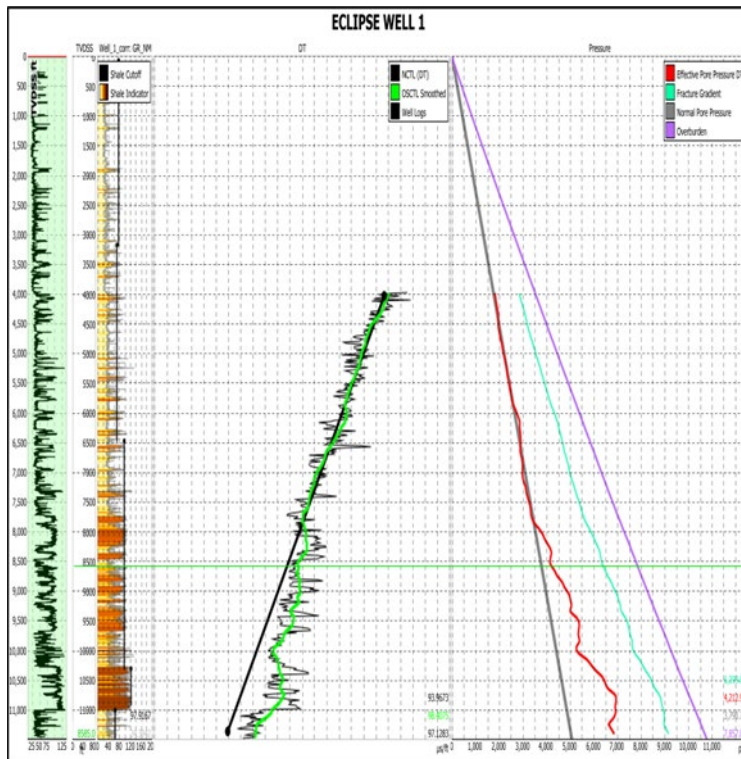


Figure 9. The pressure track in track 3 showing normal pressure, lithostatic pressure, fracture pressure and predicted pore pressure in ECL – 001.

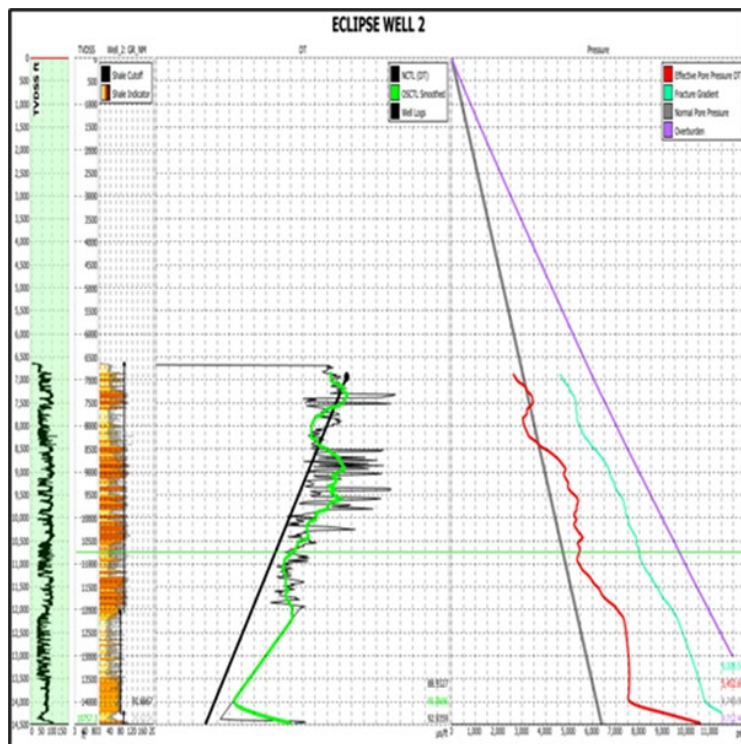


Figure 10. The pressure track in track 3 showing normal pressure, lithostatic pressure, fracture pressure and predicted pore pressure in ECL – 002.

Eclipse Well Three (ECL-003): Figure 11 shows that the observed shale compaction trend (OSCT) fits with the shale normal compaction trend at depths shallower than 8,500 ft, suggesting that these intervals are normally pressured and therefore hydrostatic. The shale sonic curve deviation from the source rock/sealing rock normal compaction trend line at depths below 8,500 ft is interpreted to indicate over-pressured intervals. At depths ranging from 11,500 – 3,000 ft, elevated in-situ pore pressures and under compaction exist which could be attributed to a secondary cause of overpressure. At 8,500 ft (onset of overpressure), geo-pressure ranges from 4,000 psi to 6,000 psi within the mildly under-compacted intervals and varies from 6,000 psi to 8,000 psi in the highly under-compacted zones. The fracture pressure in the over-pressured intervals increases with depth from 6,000 psi to 10,000 psi towards the bottom of the well.

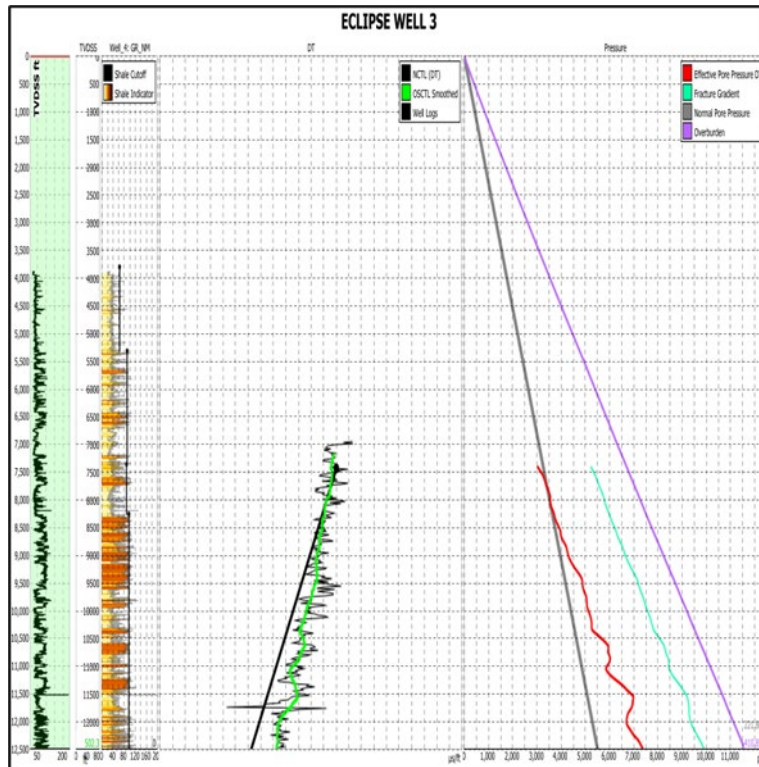


Figure 11. The pressure track in track 3 showing normal pressure, lithostatic pressure, fracture pressure and predicted pore pressure in ECL – 003.

3.4. Interpreted mud weight and casing plan

Eclipse Well One (ECL-001): The interpreted mud weight program shows four distinct levels with varying pore pressures, from which specified drilling mud weight can be interpreted and their corresponding casing plans determined (Figure 12). Drilling in the first level within 0 – 7,500 ft, should be carried out with a specified mud weight of 9.0 ppg, it is however advisable to terminate drilling at 7,000 ft and commence cementing and casing with 26 inches metal casing pipes. In the second level where elevated formation pore pressure exists, drilling should continue with a heavier mud weight of about 10.5 ppg to a depth of 9,000 ft before casing with 20 inches metal casing pipes and cementing. Between 9,000 and 10,000 ft (third level), the drilling mud is increased to a specified mud weight of 11.5 ppg and 12.25 inches metal casing pipes be used. Near the bottom of the well, which is fourth level, a drilling mud weight of 13.0 ppg is used and the open hole is eventually run by a liner (Figure 13).

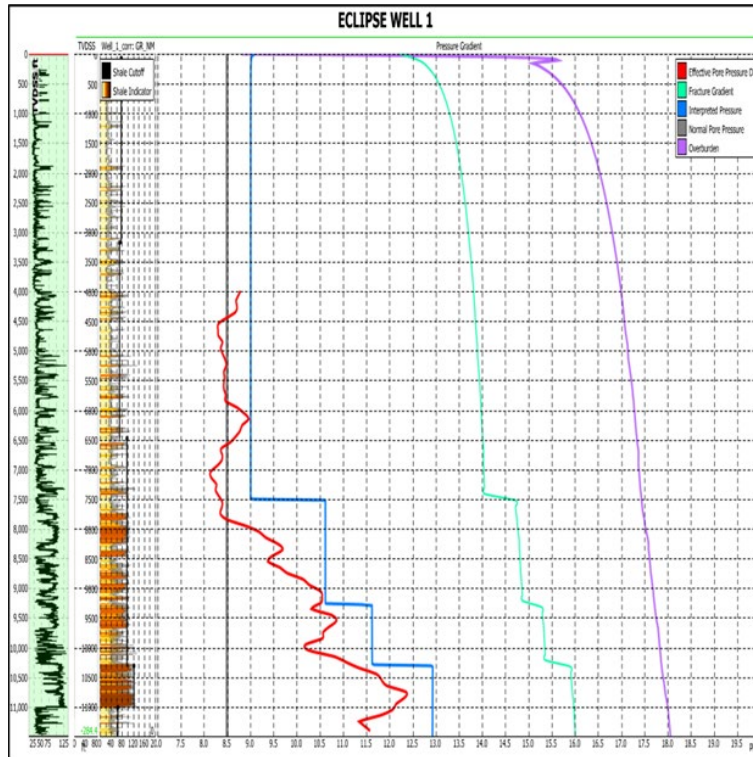


Figure 12. Equivalent mud weight plot showing four distinct levels with varying interpreted mud weights required to drill in ECL - 001.

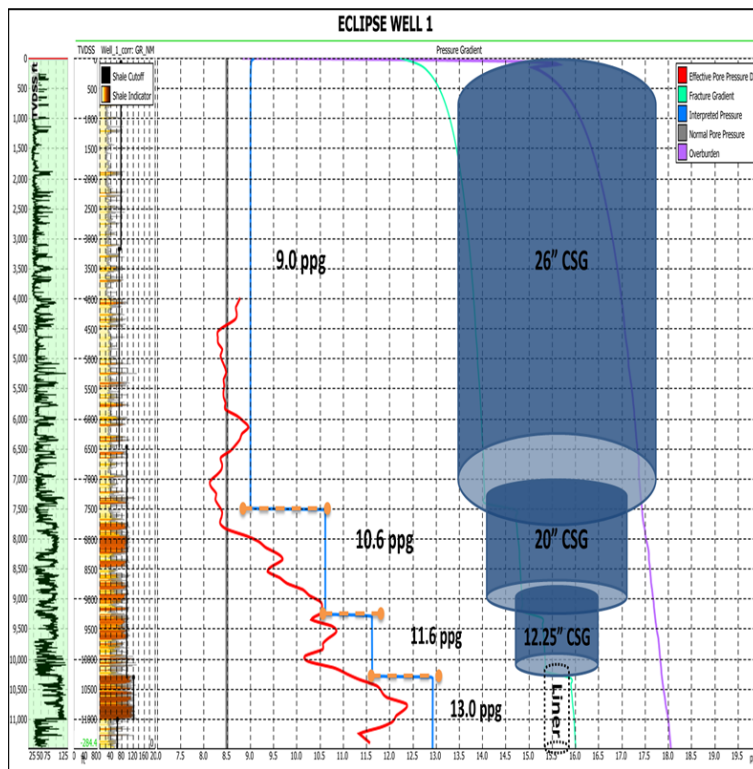


Figure 13. Drilling mud weight levels guides the planning of the casing (well architecture) to be used for drilling at varying depths in ECL - 001 well. At each level, a smaller casing pipe than the one in the level above should be used before cementing.

Eclipse Well Two (ECL-002): The abnormal pore pressure in this well started at a depth of 7,000 ft and ranges between 9.0 and 13.0 ppg. From the interpreted mud weight program, four different intervals with varying formation pore pressures and specified drilling mud weight are identified (Figure 14).

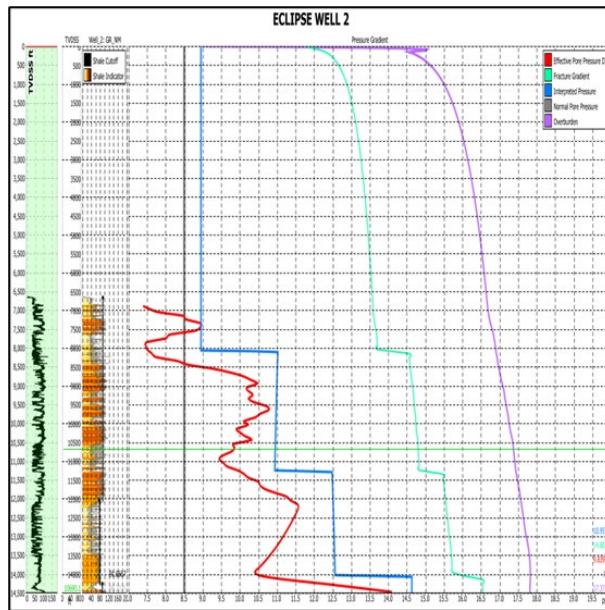


Figure 14. Equivalent mud weight plot showing four distinct levels with varying interpreted mud weights required to drill in ECL – 002.

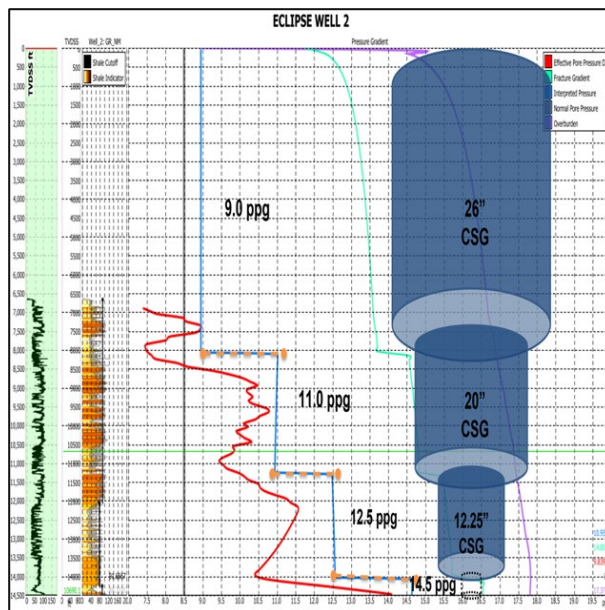


Figure 15. Drilling mud weight levels guides the planning of the casing (well architecture) to be used for drilling at varying depths in ECL – 002 well. At each level, a smaller casing pipe than the one in the level above should be used before cementing.

Drilling in the first level between 0 – 8,000 ft, should be carried out with a specified mud weight of 9.0 ppg. It is however advisable to terminate drilling at 7,000 ft and commence casing with 26 inches metal casing pipes. In the second level where elevated formation pore pressure exists, drilling mud is weighted up to 11.0 ppg before casing with 20 inches metal casing pipes and cementing. Between 11,000 and 14,000 ft in the third level, the drilling mud

density is increased and a specified mud weight of 12.5 ppg is used prior to casing and cementing. Finally, in the fourth level which is near the bottom of the well, a drilling mud weight of 14.0 ppg is used as the open hole is eventually run by a liner (Figure 15).

Eclipse Well Three (ECL-003): In this well, four unique sections with differing pore pressures were identified based on the interpreted mud weight program and the well architecture is controlled by these sections. In the first level between 0 – 7,000 ft, drilling is expected to be carried out with a specific mud weight of 9.0 ppg before casing with 26 inches metal casing pipes and cementing. In the second section (7,000 – 9,000 ft) a heavier mud weight of about 9.6 ppg should be used before casing with 20 inches casing pipes and cementing. Between 9,000 and 11,000 ft, the density of the mud is increased and a specific mud weight of 11.0 ppg is expected to be used for drilling, prior to casing with 12.25 inches casing pipes. The rest of the zones in the last sector are drilled with a drilling mud weight of 11.5 ppg.

Eclipse Well Four (ECL-004): From the equivalent mud weight plot (EMW), the normal pressure gradient is 8.5 ppg in the well, the lithostatic pressure gradient increased from the top of the well to 18.0 ppg and fracture pressure gradient is 16.0 ppg at the bottom of the well. Four distinct levels with varying formation pore pressures and specified drilling mud weight were identified based on the interpreted drilling mud program. Drilling in the first level (0–7,000 ft) of the well should be carried out with a specific mud weight of 9.0 ppg, before casing with 26 inches casing pipes and cementing. In the second level where pore pressures increase, drilling should continue with a heavier mud weight of about 10.5 ppg up to a depth of 9,500 ft before casing with 20 inches metal casing pipes and cementing. Between 9,500 and 11,500 ft in the third level, the drilling mud density is increased and a specified mud weight of 11.5 ppg should be used for drilling and 12.25 inches metal casing pipes is expected to be used for casing. Towards the bottom of the well, a drilling mud weight of 14.0 ppg should be used.

3.5. Overpressure generating mechanisms

Eclipse Well One (ECL-001): The trend of increasing compressional velocity with respect to bulk density indicates that the major cause of overpressure at depths of 7,000-10,000 ft is disequilibrium compaction. The effects of unloading which causes in-situ pore pressure to increase at a fixed overburden with decreasing effective stress in the matrix is observed at deeper depths. This is based on decreasing compressional velocity in relation to constant bulk density trend which is seen as the secondary overpressure generating mechanism (Figure 16). With the aid of a depth profile color bar to delineate depths at which these compressional velocity and bulk density data were taken, it was observed that disequilibrium compaction which causes compressional velocity and density to reach as high as 12,000 ft/s and 2.3 g/cc respectively occurred at shallower depths between 7,000 and 10,000 ft. At depths greater than 10,000 ft, unloading occurs which causes compressional velocity and density to remain constant with respect to increasing depth of burial that led to fluid expansion. The onset and effects were easily recognized by cross-plotting velocity, density and depth data for ECL-001 well (Figure 17).

Eclipse Well Two (ECL-002): From the cross-plot of compressional velocity versus bulk density (Figure 18), in ECL-002 well, it was observed that compressional velocity gradually increases up to 11,500 ft/s at 12,000 ft with respect to increasing density. This generated a trend that shows that the overpressure is caused by clay which prevents the escape of pore water during sedimentation. This cross-plot also provides further evidence of the presence of an unloading mechanism at depths greater than 12,000 ft. This could possibly be caused by an increase in pore pressure with decreasing effective stress as the secondary geo-pressure generating mechanism. In addition, the graph of cross-plot of compressional velocity, density and depth (Figure 19), clearly shows that at deeper depths, unloading effects produced a signature trend where compressional velocity dropped sharply to 8,000 ft/s at 15,000 ft and bulk density remained at a constant 2.5 g/cc with increasing overburden at the base of the well.

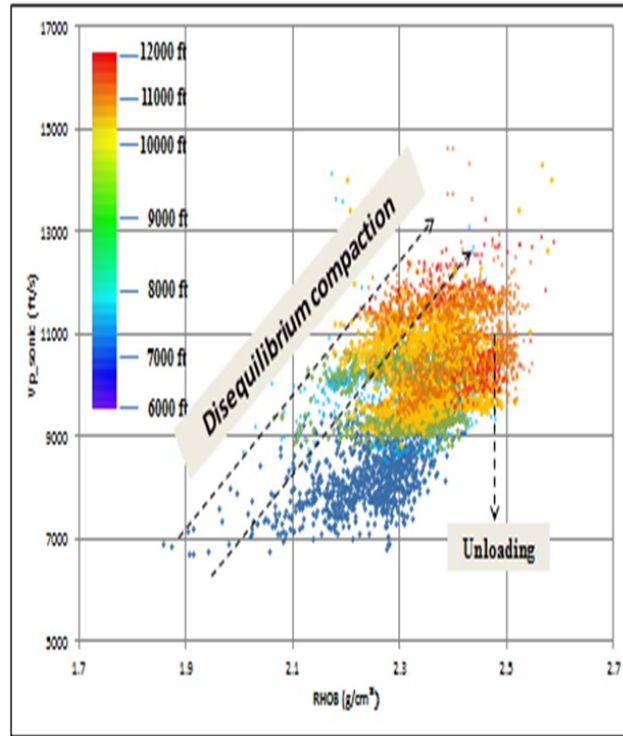


Figure 16. Cross-plot of density (g/cm^3) vs. velocity (ft/s), with a color depth bar to show a trend that describes disequilibrium compaction and unloading mechanisms as overpressure generators in ECL – 001 well.

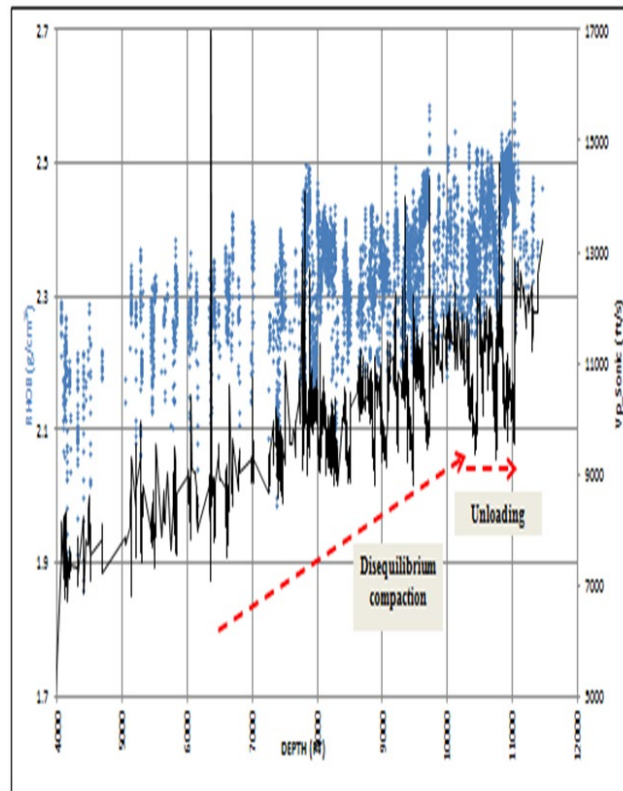


Figure 17. Cross-plot of density (g/cm^3), velocity (ft/s) vs. depth (ft) delineating intervals of increasing velocity relative to increasing density and decreasing velocity relative to constant density in ECL – 001 well.

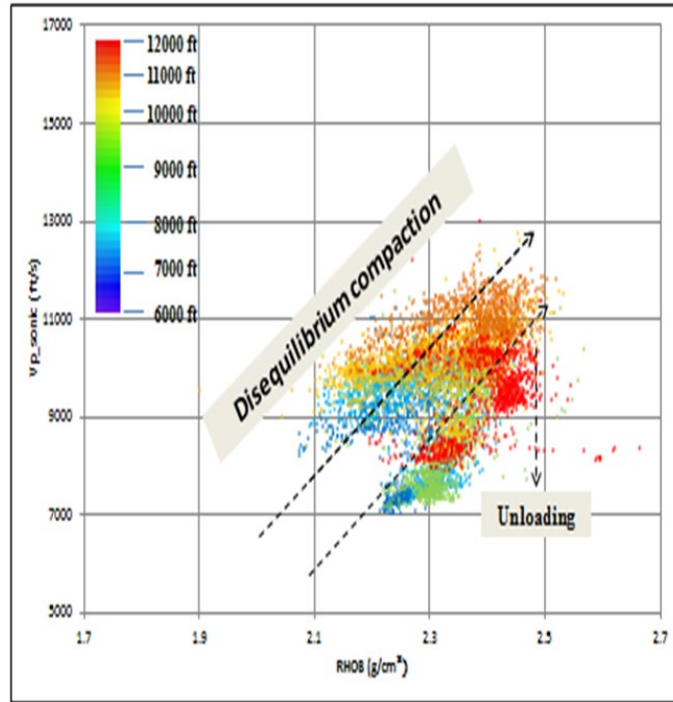


Figure 18. Cross-plot of density (g/cm^3) vs. velocity (ft/s), with a colour depth bar to show a trend that describes disequilibrium compaction and unloading mechanisms as overpressure generators in ECL – 002 well.

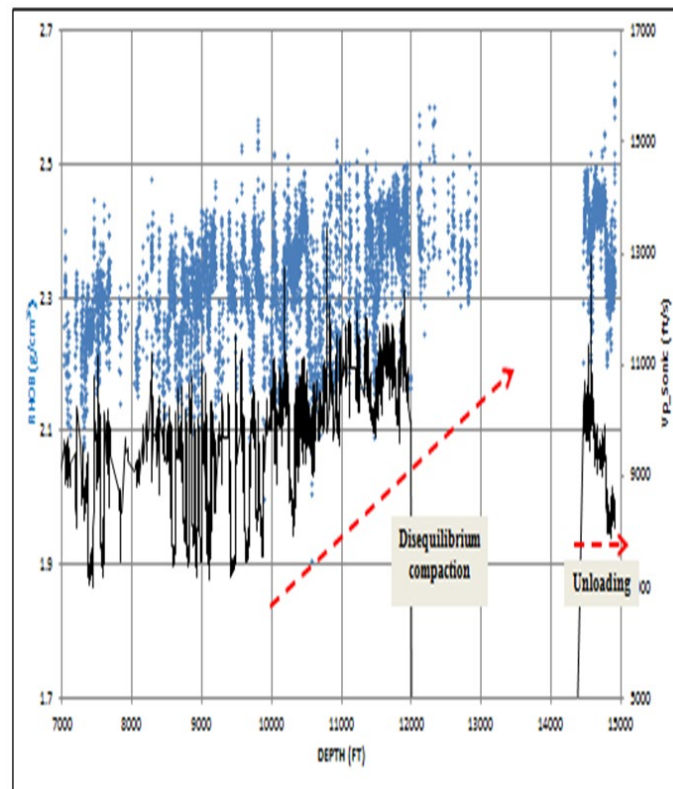


Figure 19. Cross-plot of density (g/cm^3), velocity (ft/s) vs. depth (ft) delineating intervals of increasing velocity relative to increasing density and decreasing velocity relative to constant density in ECL – 002 well.

4. Conclusions

The hydrostatic and lithostatic pressures calculated in the wells from basic pressure equations form the foundation for predicting pore pressures in the formation. These pressures are observed to increase linearly with depth and act as the minimum and maximum pressure gradients in the estimated pore pressure graphs. The hydrostatic pressure and lithostatic pressure ramp up to about 5,000 and 10,000 psi respectively in the five wells.

The Eaton's sonic/transit time and compressional velocity methods utilize equations from the Terzaghi's equation to provide a much easier way to predict geo-pressure in the wells. From this study, the use of these theoretical models show that pore pressure prediction is best carried out using the trend lines of the shales of sonic transit time logs. The deviation from the shale normal compaction trend line (NCTL) in these de-spiked logs indicates intervals of under-compaction or abnormal pressures. These shifts are more significant in deeper zones of the very deep wells representing elevated formation pore pressures.

The study shows that the onset of occurrence of overpressure in well ECL-001, well ECL-002, well ECL-003, well ECL-004 and well ECL-005 are at 8,000 ft, 8,500, 8,500 ft, 7,500 ft and 7,000 ft respectively, which implies a near regional depth overpressure. Conversion to equivalent mud weight (EMW), shows that the drilling margin falls within mud weights of 8.5 ppg and 15.0 ppg. To determine the casing plan (well architecture) required for well drilling in the Coastal Swamp Depobelt, this study indicates generally the existence of four (4) distinct levels with varying pore pressures and drilling windows (mud weights between the normal pressure and the fracture pressure), where individual levels require its own specific casing diameter after cementing to prevent fracturing.

This study shows that in the younger basins with predominant sand-shale formations like the Niger Delta Basin, the formation pore pressures at deep intervals particularly the base of the Benin Formation and the Paralic sand-shale Agbada Formation are usually over-pressured due to disequilibrium compaction. Below 12,000 ft, unloading is interpreted to cause overpressure.

Funding

The authors acknowledge the Tertiary Education Trust Fund (TETF/DR&D/CE/UNI/NSUKKA/BR/2024/VOL.1), University of Nigeria, Nsukka for the sponsorship of this research.

References

- [1] Doust H and Omatsola E. Niger Delta. In: J.D. Edwards and P.A. Santogrossi (eds.), Divergent/passive margin basins: American Association of Petroleum Geologists Memoir, 1990; 48: 239 - 248.
- [2] Terzaghi K. Peck RB and Mesri G. Soil Mechanics in Engineering Practice (3rd Edition). John Wiley & Sons publishers, 1996.
- [3] Sen S and Ganguli SS. Estimation of pore pressure and fracture gradient in volve field, Norwegian North Sea. In: SPE oil and gas India conference and exhibition, 2019. <https://doi.org/10.2118/194578> .
- [4] Ganguli SS and Sen S. Investigation of present-day in-situ stresses and pore pressure in the south Cambay Basin, western India: implications for drilling, reservoir development and fault reactivation. Marine and Petroleum Geology, 2020; 118: 104422.
- [5] Radwan AE and Sen S. Stress path analysis for characterization of in situ stress state and effect of reservoir depletion on present-day stress magnitudes: reservoir geomechanical modeling in the Gulf of suez rift basin, Egypt. Natural Resources and Reserves, 2020. <https://doi.org/10.1007/s11053-020-09731-2>
- [6] Atake-Enade C, Antia M, Koikoibo J and Odhomor K. Wellhead Woes: A special report on the wellhead blowout from Aiteo's OML 29 Well 1, Nembe, Bayelsa State, Nigeria. Health of Mother Earth Foundation (HOMEF), 2021. <https://homef.org/wp-content/uploads/2021/12/well-head-woes-single-pages.pdf>
- [7] Knox G and Omatsola ME. Development of the Cenozoic Niger Delta in terms of the escalator regression model and Impact on Hydrocarbon Distribution. In: W.J.M. vander Linden et al. (eds.), Proceedings of KNGMG Symposium on Coastal Lowlands, Geology, Geotechnology, Kluwer Academic Publishers, Dordrecht, 1989; 181-202.

- [8] Evamy BD, Haremboure J, Kameling P, Knaap W A, Molloy F A and Rowlands P H. Hydrocarbon habitat of Tertiary Niger Delta: American Association of Petroleum Geologists Bulletin, 1978; 62: 1 – 39.
- [9] Avbovbo AA. Tertiary Lithostratigraphy of Niger Delta. American Association of Petroleum Geologists Bulletin, 1978; 62: 295-300.
- [10] Anyiam OA, Utoh MC, Moghalu OA and Jolly BA. Maximizing Production Through Evaluation of New Prospects in the Producing “Tuba Field”, Onshore Niger Delta. Petroleum and Coal, 2020; 62(2): 577-586.
- [11] Doust H and Omatsola E. Niger Delta. AAPG Memoir, 1989; 48: 201–238.
- [12] Chilingar G, Robertson J and Riekeiii H. Origin of abnormal formation pressures. Developments in Petroleum Science, 2002; 50: 21 - 67.
- [13] Nosike L. Exploration and Production Geoscience. Comprehensive skills acquisition for an evolving industry. Delizon publishers, 2020; 237 - 245.
- [14] Eaton BA. The equation for geopressure prediction from well logs. Society of Petroleum Engineers of AIME, 1975; Paper SPE 5544.
- [15] Matthews WR and Kelly J. How to predict formation pressure and fracture gradient. Oil and Gas Journal, 1967; 65: 92 - 106.
- [16] Ozumba B. Geology of the Niger Delta: An Overview for Geophysics Processors. An SPDC presentation for geologists in Nigeria, 2013.
- [17] Swarbrick RE. Review of pore-pressure prediction challenges in high-temperature areas. The Leading Edge, 2012; 31(11): 1288-1294. <https://doi.org/10.1190/tle31.111288.1>
- [18] Hoesni J. Origins of overpressure in the Malay Basin and its influence on petroleum systems, Durham, PhD thesis, University of Durham, 2004.

To whom correspondence should be addressed: prof. O. A. Anyiam, Department of Geology, University of Nigeria, Nsukka, Nigeria, E-mail: okwudiri.anyiam@unn.edu.ng